Technische Informationsbibliothek
- Dokumentlieferung
Postfach 6080
30060 Hannover

Tel: 0511 / 762-8989
Fax: 0511 / 762-8998
E-Mail: customerservice@tib.uni-hannover.de

06.01.2015

Bibliothek Chemie/Physik
der Universitaetsbibliothek Leipzig
Frau Johanna Zander
Johannisallee 29
04103 Leipzig

SUBITO-Dokumentenlieferung - Lieferschein (Bitte Rechnung abwarten)

Angaben zur Lieferung

Bestellnummer: SUBITO:VF15010600687 / E000474963
Versanddatum: 06.01.2015
Versandart und -weg: FAX
Lieferadresse: chembib@rz.uni-leipzig.de
Bestellart: Normal
Kommentar:

Angaben zum bestellten Dokument

Signatur: ZZ 247/1 [Haus2]
Zeitschriftentitel: Physics of the solid state
Jahrgang/Heft: VOL 54, NUMB 9
Erscheinungsjahr: 2012
Seiten: 1751-1763
Autor: Mirsagatov, S. A.; Uteniyazov, A. K.; Ac
Artikel: Mechanism of current transport in Schottky barrier diodes based on coarse-grained CdTe films

Kundendaten

Ihre Kundennummer der Lieferbibliothek: K000807199 Kundengruppe: 4
Ihr Aktenzeichen:
Ihre Bemerkung zur Bestellung: 2015-4

Wir weisen Sie als Empfänger darauf hin, dass Sie nach geltendem Urheberrecht die von uns übersandten Vervielfältigungsstücke ausschließlich zum privaten oder sonstigem eigenen Gebrauch verwenden und weder entgeltlich noch unentgeltlich in Papierform oder als elektronische Kopie verbreiten dürfen.

ISSN 1063-7834, Physics of the Solid State, 2012, Vol. 54, No. 9, pp. 1751–1763. © Pleiades Publishing, Ltd., 2012.
Original Russian Text © Sh.A. Mirsagatov, A.K. Uteniyazov, A.S. Achilov, 2012, published in Fizika Tverdogo Tela, 2012, Vol. 54, No. 9, pp. 1643–1654.

SEMICONDUCTORS

Mechanism of Current Transport in Schottky Barrier Diodes Based on Coarse-Grained CdTe Films

Sh. A. Mirsagatov[a, *], A. K. Uteniyazov[b, **], and A. S. Achilov[a]

[a] *Physical-Technical Institute, Uzbekistan Academy of Sciences, ul. G. Mavlyanova 2B, Tashkent, 700084 Uzbekistan*
** e-mail: mirsagatov@rambler.ru*
[b] *Berdakh Kara-Kalpak State University, ul. Akademika Abdirova 1, Nukus, Uzbekistan*
*** e-mail: abat-62@mail.ru*

Received February 29, 2012

Abstract—The possibility of fabricating a Schottky barrier on Al–*p*-CdTe structures with the lowest density of surface states has been demonstrated and confirmed by the results obtained from the capacitance–voltage and photoelectric measurements of the potential barrier height. It has been established that, at different forward bias voltages, there are different exponential dependences of the electric current on the voltage, which are related to the changes in kinetic parameters of the base of the Al–*p*-CdTe–Mo structure. It has been shown that the Al–*p*-CdTe–Mo structure at a forward current and high illumination levels operates as an injection photodiode. This injection photodiode has a high current sensitivity. When the current is switched on in the reverse direction, after the complete coverage of the base of the structure by the space charge, electrons responsible for the charge transfer mechanism and noise characteristics of the structure are injected from the rear contact.

DOI: 10.1134/S1063783412090193

1. INTRODUCTION

In recent years, detectors with a Schottky barrier based on CdTe and $Cd_{1-x}Zn_xTe$ have been intensively developed [1–3]. Significant advantages of these detectors are small dark reverse currents ($\sim 10^{-7}$ A) and high operating temperatures ($T \geq 300$ K). Furthermore, detectors based on Schottky barrier diodes can be used for detection of high-energy photons with energies up to 1 MeV and higher with a limiting energy resolution without a special circuit for processing an electrical signal in the detector circuit [4]. However, single crystals of II–VI compounds used to fabricate nuclear radiation detectors have disadvantages. The main disadvantage of II–VI single crystals is that they contain a significant number of defects of different nature which decrease the lifetime of charge carriers and deteriorate the performance characteristics of detectors [5]. Some of the disadvantages can be eliminated if coarse-grained polycrystalline CdTe films with a columnar structure of grains (crystallites) are used as the base material. In these films, grains permeate them over the entire thickness. The advantage of these polycrystalline films is that they exhibit properties of single crystals in the growth direction and properties of polycrystals in the horizontal direction. The grain boundaries are sinks for defects of different types, which leads to an increase in the lifetime of charge carriers in the crystallites [6]. On the other hand, these boundaries can shunt crystallites and serve as the main source of leakage current. Therefore, the passivation of grain boundaries is of paramount importance for polycrystalline semiconductor materials used in the fabrication of solid-state electronic devices. We have developed a technology [7] that makes it possible to fabricate high-resistivity coarse-grained polycrystalline CdTe films with sufficiently high values of the lifetimes ($\tau \sim 10^{-7}$–10^{-6} s) of minority charge carriers.

The purpose of this work is to fabricate structures with a Schottky barrier based on CdTe films of this type and to investigate the charge transfer mechanism in them in order to understand the physical processes occurring in these structures and to evaluate the possibilities for their use in instrument development.

2. SAMPLE PREPARATION AND EXPERIMENTAL TECHNIQUE

Film structures with a Schottky barrier were fabricated by means of the deposition of aluminum in a vacuum ($\sim 10^{-5}$ Torr) on the surface of coarse-grained CdTe films with *p*-type conductivity. The rear contact was prepared from molybdenum. The *p*-CdTe films had an electrical resistivity $\rho \approx 10^5$–3×10^7 Ω cm and a minority carrier lifetime of $\sim 10^{-7}$–10^{-6} s. The films had a columnar structure of grains in the growth direction and represented almost a single crystal. The grain sizes in the cross section ranged from 100 to 150 μm. The thickness of the *p*-CdTe films was 40–50 μm, so

TIB HANNOVER +495117628998 Tue Jan 6 16:57:41 2015 Seite 3 von 14

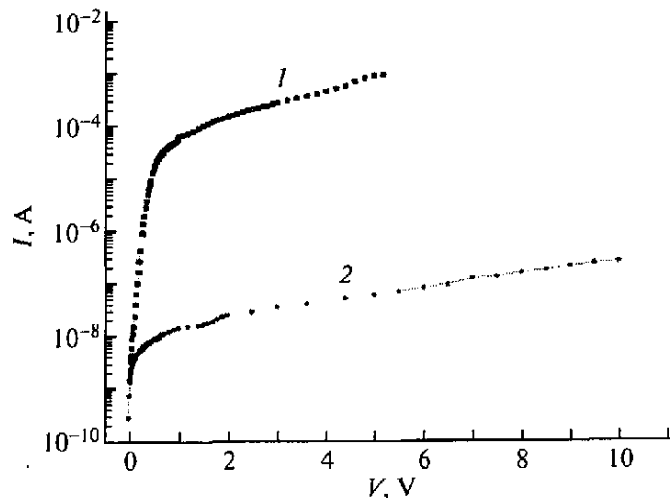

Fig. 1. (*1*) Forward and (*2*) reverse branches of the current–voltage characteristic of the Schottky barrier diode (Al–*p*-CdTe–Mo) with a base resistivity $\rho \approx 10^7\ \Omega$ cm on a semilogarithmic scale at room temperature.

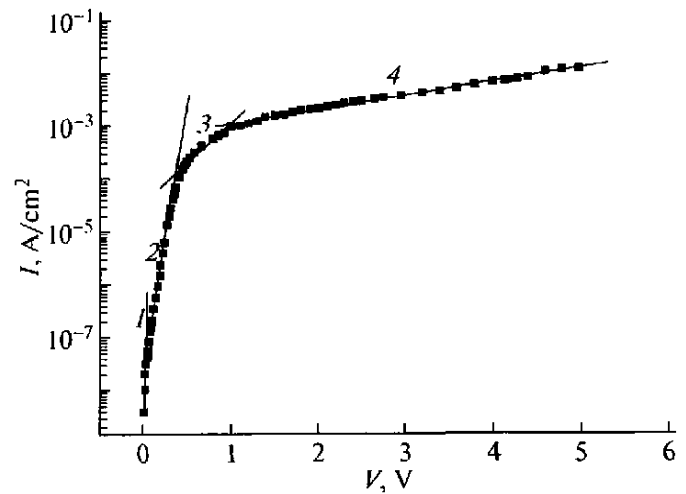

Fig. 2. Forward branch of the current–voltage characteristic of a typical Schottky barrier diode (Al–*p*-CdTe–Mo) with a base resistivity $\rho \approx 10^7\ \Omega$ cm on a semilogarithmic scale in the dark at $T = 300$ K. The aluminum contact area is $S \approx 0.07$ cm^2. Numerals indicate different portions of the dependence.

that the grains permeated the films throughout the thickness. The films were compensated materials.

The current–voltage characteristics of the fabricated structures were measured in the forward and reverse directions of the current in the dark and the light at room temperature. The structures were illuminated by laser radiation with a power density of 83 mW/cm^2 and a wavelength 0.625 μm. The capacitance–voltage $C(V)$ characteristics were measured at a frequency of 100 kHz, because they had an identical shape in the frequency range from 100 kHz to 5 MHz.

The constant lifetime of minority carriers (τ_n) was determined using the photoelectric method and from the relaxation of an electrical signal at a voltage V_{cc} (idling mode) [8, 9]. The photoelectric measurements of the lifetime of minority carriers τ_n were performed using light diodes emitting at wavelengths of 0.54 and 0.69 μm. On these light-emitting diodes, we fed U-shaped pulses with a duration of the order of 100 μs and a pulse edge steepness of no more than 2×10^{-8} s. The interval between the U-shaped pulses was of the order of 10^{-4}–10^{-3} s.

When the lifetime of minority carriers τ_n was measured using the relaxation of an electrical signal, U-shaped pulses with an amplitude of 60–80 mV and a duration of 100–200 μs were fed from a G5-53 calibrated pulse generator. The duration of the pulse leading edge was no more than 2×10^{-8} s, and the interval between the pulses was no less than 5×10^{-4} s.

3. EXPERIMENTAL RESULTS AND DISCUSSION

Figure 1 shows the forward and reverse branches of the current–voltage characteristic of a typical Schottky barrier diode (with a base resistivity $\rho \approx 10^7\ \Omega$ cm) on a semilogarithmic scale. The current direction in the structure was considered to be forward when a positive potential was applied to the Mo contact. The general analysis of the current–voltage characteristics has demonstrated that the structure exhibits rectifying properties and that the rectification coefficients, which are determined as the ratio between the forward and reverse currents at a fixed voltage $K = I_{forw}/I_{rev}$ ($V = 5$ V), account for more than four orders of magnitude (Fig. 1).

3.1. Analysis of the Forward Branch of the Current–Voltage Characteristics

First and foremost, we analyze the forward branch of the current–voltage characteristic of a typical sample of Schottky barrier diodes measured at a direct current in the dark at room temperature (Fig. 2). As can be seen from Fig. 2, the forward branch of the current–voltage characteristic consists of four portions, which are described by the following exponential relationships: (*1*) $I = I_{01}[\exp(qV/c_1kT) - 1]$, where $c_1 = 1.03$ and $I_{01} = 4 \times 10^{-10}$ A; (*2*) $I = I_{02}[\exp(qV/c_2kT) - 1]$, where $c_2 = 1.86$, and $I_{02} = 1.1 \times 10^{-9}$ A; (*3*) $I = I_{03}[\exp(qV/c_3kT) - 1]$, where $c_3 = 14.8$ and $I_{03} = 6 \times 10^{-6}$ A; and (*4*) $I = I_{04}[\exp(qV/c_4kT) - 1]$, where $c_4 = 60$ and $I_{04} = 4.1 \times 10^{-5}$ A.

In portion *1* of the forward branch of the current–voltage characteristic, the electric current in the structure is most probably limited by the thermionic emission [10], because the ideality factor has the value $c_1 = 1.03$, i.e., it is approximately equal to unity, and the

TIB HANNOVER +495117628998 Tue Jan 6 16:57:41 2015 Seite 4 von 14

potential barrier height is $W = 0.95$ K according to the calculation from the formula $I_0 = A^* T^2 \exp(-W/kT)$ for values of the Richardson constant $A^* = 49$ A/cm² K² and $T = 300$ K. The value of A^* is estimated from the following formula [10]: $A^* = (4\pi q m_p^* k^2)/h^3$, where $m_p^* = 0.41 m_0$ is the hole effective mass [11]. It is known that the height of the potential barrier between the metal and the semiconductor depends on the difference in the work functions of the metal and the semiconductor. According to the data presented in [12], the work function of aluminum lies in the range from 2.98 to 4.36 eV, and its value is determined primarily by the state of the metal surface. The work function of the semiconductor is determined as the sum of the electron affinity (χ_s) and the energy at the Fermi level (E_F). In order to estimate the value of E_F, the concentration of equilibrium holes (p_0) was determined from the capacitance–voltage characteristic plotted in the C^{-2}–V coordinates (Fig. 3). The steep portion *1* of the dependence $C^{-2} = f(V)$ (Fig. 3) is described by two straight lines. This indicates the heterogeneity of the near-surface region of the p-CdTe film. The concentrations of equilibrium holes were calculated from the slopes of these straight lines according to the formula [13]

$$p_0 = (2/q\varepsilon\varepsilon_0 S^2)(dV/dC^{-2}). \qquad (1)$$

The concentrations thus obtained are equal to 6.4×10^{11} and 1.4×10^{13} cm⁻³, respectively. When the dependence $C^{-2} = f(V)$ is extrapolated by a straight line, the intersection with the voltage axis at $C^{-2} \longrightarrow 0$ takes place at the point $V = -1.02$ V (Fig. 3). The concentrations $p_{01} = 6.4 \times 10^{11}$ cm⁻³ and $p_{02} = 1.4 \times 10^{13}$ cm⁻³ correspond to the energies at the Fermi level $E_{F1} = 0.4$ eV and $E_{F2} = 0.32$ eV, respectively, and the electron affinity of cadmium telluride is $\chi_s = 4.28$ eV [12]. Since the work function for a p-type semiconductor can be written as $\varphi_S = \chi_s + (E_g - E_F)$, we find that $\varphi_{S1} = 5.36$ eV at $p_{01} = 6.4 \times 10^{11}$ cm⁻³ and $\varphi_{S2} = 5.56$ eV at $p_{02} = 1.4 \times 10^{13}$ cm⁻³. For the ideal contact between the metal and the p-type semiconductor, the potential barrier height with due regard for the lowering of the barrier by the value $\Delta(q\varphi)$ due to the Schottky effect is determined by the formula [10]

$$\varphi_n = E_g - q(\varphi_m - \chi_s) - \Delta(q\varphi). \qquad (2)$$

Since the high-resistivity layer with the effective acceptor concentration $N_{A1} = 6.4 \times 10^{11}$ cm⁻³ is directly in contact with the metal (Al), it is this layer that is responsible for the formation of the potential barrier. On this basis, we will further consider the potential barrier φ_n formed between this CdTe layer and Al. According to the data obtained from the photoelectric measurements [14], the band gap of the cubic modification of CdTe is $E_g = 1.49$ eV at $T = 300$ K.

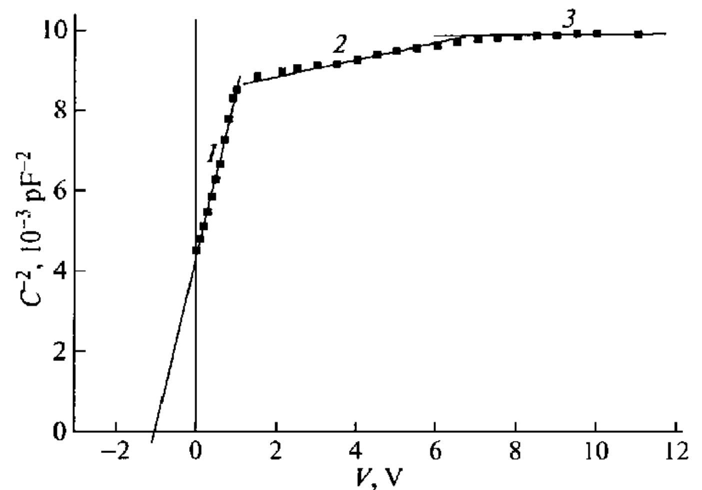

Fig. 3. Capacitance–voltage characteristic of a typical sample of Schottky barrier diodes with a base resistivity $\rho \approx 10^7$ Ω cm at the reverse bias in the C^{-2}–V coordinates at a frequency of 100 kHz. Numerals indicate different portions of the dependence.

The decrease in the barrier height, according to the calculation from the formula [10]

$$\Delta\varphi = (q\xi/4\pi\varepsilon\varepsilon_0)^{1/2}, \qquad (3)$$

is equal to 9.3×10^{-3} V at the effective concentration of acceptor centers $N_{A1} = 6.4 \times 10^{11}$ cm⁻³. In the evaluation of $\Delta\varphi$, the maximum value of the field strength ξ in the depletion layer was found using the formula

$$\xi = [2qN_A(V_D - V_a)\varepsilon\varepsilon_0]^{1/2}. \qquad (4)$$

Thus, we obtained $\varphi_n = 1.38$ eV for the parameters $E_g = 1.49$ eV, $\varphi_m = 4.36$ eV (for Al), $\chi_s = 4.28$ eV, and $\Delta\varphi = 9.3 \times 10^{-3}$ V. This value of φ_n is ~0.4 eV higher than the potential barrier height determined from the pre-exponential factor I_{01} of the current–voltage characteristic.

Let us now consider the agreement between the calculated value of the potential barrier height φ_n and the values determined using the capacitance–voltage characteristic and the photoelectric method. By using the capacitance–voltage characteristic, the potential barrier height is determined from the following expression [10]:

$$\varphi_n = V_i + V_p + (kT/q) - \Delta\varphi, \qquad (5)$$

where V_i is the point of intersection of the dependence $C^{-2}(V)$ with the voltage axis at $C^{-2} \longrightarrow 0$, which is equal to -1.02 eV for the sample under investigation (Fig. 3); qV_p is the difference between the energies at the Fermi level and the valence band top, which is equal to 0.4 eV for the sample under investigation; and

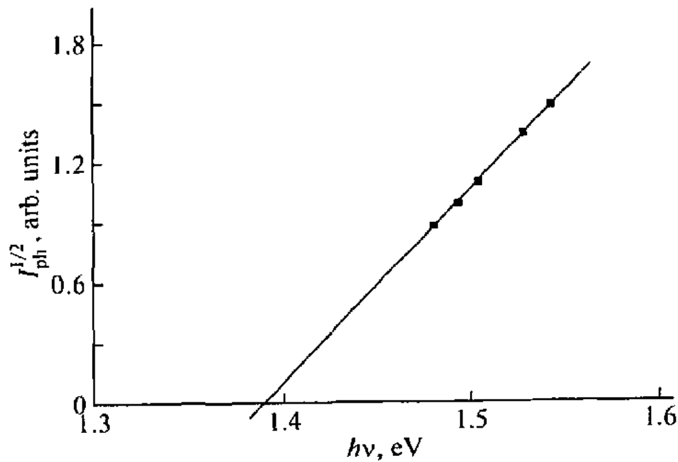

Fig. 4. Dependence of the photocurrent $I_{ph}^{1/2}$ (in relative units) above the fundamental absorption edge on the photon energy $h\nu$.

$(kT/q) = 2.58 \times 10^{-2}$ V at $T = 300$ K. Based on these data, from expression (3) we find the potential barrier height $\varphi_n \approx 1.4$ eV. This value almost completely coincides with the calculated value, which was obtained taking into account the lowering of the potential barrier under the action of the space charge field and image forces.

The height of the potential barrier was also determined using the photoelectric method. It is the most direct and accurate method for determining the height of the potential barrier [10]. When the sample is illuminated on the metal side by a monochromatic light with an energy $h\nu > q\varphi_n$, electrons are excited in the metal with an energy high enough to overcome the potential barrier; in this case, the dependence of the photoresponse or photocurrent on the energy of incident photons is described by the relationship [12]

$$I_{ph}^{1/2} \sim h\nu - q\varphi_n. \qquad (6)$$

The dependence of the square root of the photocurrent on the photon energy is a straight line (Fig. 4). By extrapolating this straight line to the energy axis, we find the height of the energy barrier $\varphi_n \approx 1.39$ eV, which coincides with the calculated value. Good agreement between the calculated and experimental values of the energy barrier height φ_n shows that the Schottky barrier between Al and p-CdTe is formed almost without surface states. It seems likely that, in this case, an important role is played by the thin layer of aluminum oxide (Al_2O_3) [12], which is formed during the deposition of aluminum on the surface of the p-CdTe film. It is known [12] that oxide layers of the SiO_2 and Al_2O_3 types are characterized by ionic bonds and, on their surfaces, surface states are not formed; consequently, they effectively passivate surface states of semiconductors with covalent bonds.

At current densities $J = 3.3 \times 10^{-7}$–5.5×10^{-5} A cm^{-2} (Fig. 2) in the structure under investigation, the current as a function of the voltage is described by the exponential relationship, in which the factor in the exponent c is equal to approximately two and the pre-exponential factor is $J_0 = 2.7 \times 10^{-8}$ A cm^{-2} (Fig. 2, straight line *2*). The value of c in the exponent is often equal to two in the case where the current in the structure is limited by the recombination of charge carriers in the space charge layer [15]. In wide-band-gap semiconductors (especially, at low temperatures), the recombination of charge carriers in the forward current direction can be rather significant. The concentration of charge carriers, including nonequilibrium charge carriers, in the space charge layer varies very greatly (by a factor of e) at a distance l, where the potential changes by kT/q. Since, at a sufficiently low injection level, the recombination rate is determined by the product of the concentrations of electrons and holes, i.e., $n \cdot p$, the highest rate of recombination will be in the region where $p \approx n$, i.e., at the boundary between the p- and n-regions. It can be demonstrated that the majority of charge carriers in the space charge layer recombine in a layer with a thickness $\sim l$ near the geometrical boundary of the Al–p-CdTe structure with the Schottky barrier. The quantity $l = kT/qE_{max}$ (where E_{max} is the maximum electric field strength) is similar to the diffusion displacement length in neutral regions. The maximum electric field strength of $\sim 4.84 \times 10^2$ V/cm in the sample under investigation, according to [10], is generated at a distance $l \approx (q/16\pi\varepsilon\varepsilon_0 E_{max})^{1/2} \approx 6 \times 10^{-6}$ cm from the geometrical boundary of the Al–p-CdTe structure.

The recombination current can be represented in the form [15]

$$I_r = qn(0)l/2\tau_0 = n_i(kT/2E_{max}\tau)\exp(qV/2kT) = I_0\exp(qV/2kT), \qquad (7)$$

where $n(0)$ is the concentration of charge carriers at the metal–semiconductor interface. By using the experimental value $J_{02} = 1 \times 10^{-8}$ A cm^{-2} and its analytical expression, from relationship (7) we find the lifetime $\tau \approx 3 \times 10^{-9}$ s for the parameters $n_i = 5 \times 10^6$ cm^{-3}, $E_{max} = 4.8 \times 10^2$ V/cm, and $T = 300$ K. The estimated lifetime ($\tau \approx 3 \times 10^{-9}$ s) is of almost the same order of magnitude as the values of the times determined from the relaxation of photoconductivity at current densities corresponding to portion *2* of the current–voltage characteristic (Fig. 2). The photoconductivity relaxation curve is described by two exponential dependences. The lifetimes determined from these dependences are equal to $\sim 1.3 \times 10^{-8}$ and $\sim 8.0 \times 10^{-8}$ s. The difference between the values of the charge carrier lifetimes calculated from the pre-exponential factor and from the relaxation of photoconductivity is less than one order of magnitude. This circumstance is explained by the fact that the recombination processes

TIB HANNOVER +495117628998 Tue Jan 6 16:57:41 2015 Seite 6 von 14

are involved not only simple recombination centers but also complex centers [16] into which the charge carriers are trapped. In this case, the recombination rate can be written as

$$U = N_R \frac{c_n c_p (np - n_i^2)}{c_n(n + n_1) + c_p(p + p_1) + a\tau_i np}, \qquad (8)$$

where N_R is the concentration of recombination centers (complexes); n and p are concentrations of electrons and holes, respectively; n_i is the intrinsic concentration in the semiconductor; c_n and c_p are the trapping coefficients of electrons and holes, respectively; n_1 and p_1 are the equilibrium concentrations of electrons and holes, respectively, under the conditions where the Fermi level coincides with the impurity level (the so-called static Shockley–Read factors); τ_i is the time accounting for the inertia of various processes involving the electronic exchange within the recombination complex; and a is the coefficient dependent on the particular type of defect–impurity or impurity complexes (see [16]). A similar law of the recombination is possible not only in the aforementioned cases but also in semiconductors with developed recombination-stimulated rearrangements of metastable recombination complexes of the "negatively charged acceptor–positively charged interstitial ion" or "positively charged donor–negatively charged vacancy" type [17]. A similar pattern can also be obtained for II–VI semiconductors, in which the excitation is accompanied by chemical reactions that lead to the decay of complex centers of the shallow donor–vacancy type [18]. Despite the differences observed in the aforementioned cases, they are characterized a general feature: the recombination of nonequilibrium electrons and holes occurs with a delay, and the inclusion of the inertia of the electronic exchange within the recombination complex leads to the appearance of the last term in the denominator of formula (8), which at a sufficiently high excitation level can be decisive.

In cadmium telluride, cadmium atoms represent a volatile component. Therefore, in the sublattice of cadmium atoms, singly and doubly charged vacancies of cadmium atoms, V_{Cd}^- and V_{Cd}^{2-}, and an interstitial atom Cd_i are readily formed. In the majority of cases, doubly charged vacancies of cadmium atoms V_{Cd}^{2-} form complexes with positively charged impurities of the $(V_{Cd}^{2-}D^+)^-$ type and neutral interstitial tellurium atoms of the $(V_{Cd}^{2-}Te_i^*)^{2-}$ type [19]. These complexes are deep acceptor centers. In cadmium telluride, there are donor impurities (Cl, In, Al) and acceptor impurities (P, Li, Ag, Au, Cu). Atoms of silver, copper, and gold can generate deep acceptor centers. Probably, these defects and impurities can form defect–impurity complexes of the "negatively charged acceptor–positively charged interstitial ion" or "positively charged donor–negatively charged vacancy" type, through which the recombination of nonequilibrium charge carriers occurs with a delay. Apparently, these complexes at high current densities play a decisive role in the recombination processes occurring in the base layers (p-CdTe) of the structure under investigation.

As was noted above, the difference between the calculated and experimental values of the charge carrier lifetime τ is not too large (less than one order of magnitude). This indicates that the recombination processes occur with the participation of complex recombination centers; however, they do not play a decisive role. In this case, the denominator of expression (8) includes the condition

$$c_n(n + n_1) + c_p(p + p_1) \approx a\tau_i np. \qquad (9)$$

As regards the two values of the time on the relaxation curve, this circumstance is explained by the fact that, in the base layer (p-CdTe) of the structure under investigation, there are at least two types of complexes, one of which with a lifetime of $\sim 1.3 \times 10^{-8}$ s makes a significant contribution to the recombination processes.

Since the increase in the recombination current with an increase in the bias voltage occurs more slowly as compared to the diffusion current, the forward current at sufficiently high bias voltages will increasingly be determined by the processes occurring in the quasi-neutral regions of the base. In this case, the applied bias voltage will be redistributed between the barrier and the quasi-neutral part of the base, which is reflected in the value of the factor c in the exponent. The factor c can have different values depending on the ratio of the thickness of the base (d) to the diffusion length of minority carriers (L_n). Stafeev calculated the current–voltage characteristics for this phenomenon under the conditions where the current is limited by the recombination in the quasi-neutral part of the base. As a result, this author obtained the following relationship [20]:

$$I = I_0 e^{qV/ckT}, \qquad (10)$$

where

$$C = \frac{2 + b\cosh\frac{d}{L_n} + b}{b + 1},$$

$$I_0 = \frac{kT}{2q(b+1)}\frac{S}{\rho L_n}\frac{\cosh\frac{d}{L_n}}{\tan\left(\frac{d}{2L_n}\right)}. \qquad (11)$$

Here, $b = \mu_n/\mu_p$ is the ratio between the mobilities of electrons and holes. Probably, potions *3* and *4* (Fig. 2) of the current–voltage characteristic can be described by relationship (10), because, in these cases, the values of the factor c in the exponent are considerably larger than 2, or, more precisely, they are equal to 14.8 and

TIB HANNOVER +495117628998 Tue Jan 6 16:57:41 2015 Seite 7 von 14

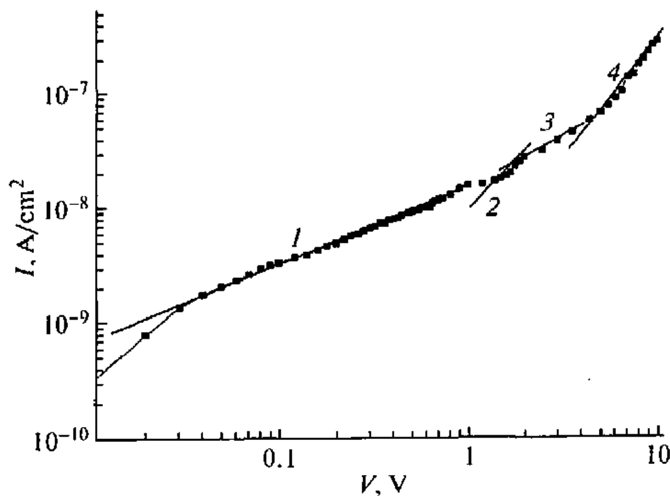

Fig. 5. Current–voltage characteristic of a typical reverse-biased Schottky barrier diode with a base resistivity $\rho \approx 10^5\ \Omega$ cm on a log–log scale: (*1*) $I \sim V^{0.6}$, (*2, 4*) $I \sim V^2$, and (*3*) $I \sim V$.

60.0, respectively. In these portions of the current–voltage characteristic, we also determined the pre-exponential factor, which was equal to 6×10^{-6} A for portion *3* and 4.1×10^{-5} A for portion *4*. By using the experimental data presented above and relationships (10) and (11), we determined the values of the diffusion length of minority carriers (electrons) L_n, the product of the mobility by the lifetime of electrons $\mu_n\tau_n$, and the base resistivity ρ. These parameters of the current–voltage characteristic had the following values: $L_n \approx 14.7$ μm, $\mu_n\tau_n \approx 8.3 \times 10^{-5}$ cm^2/V, and $\rho \approx 4.7 \times 10^6\ \Omega$ cm for portion *3* and $L_n \approx 10.3$ μm, $\mu_n\tau_n \approx 4.1 \times 10^{-5}$ cm^2/V, and $\rho \approx 3 \times 10^6\ \Omega$ cm for portion *4* with the values of $d \approx 50$ μm, $b = \mu_n/\mu_p = 10$, and $T = 300$ K. In these portions of the current–voltage characteristic, we also measured the values of the photoconductivity relaxation, which are described by the exponential dependence well approximated by two straight lines. From the slopes of the straight lines of the dependence $\ln I \sim \ln V – t/\tau$ in portion *3* of the current–voltage characteristic, we determined $\tau_1 \approx 8.7 \times 10^{-7}$ s and $\tau_2 \approx 1.4 \times 10^{-6}$ s. For portion *4* of the current–voltage characteristic, we obtained $\tau_1 \approx 9.1 \times 10^{-7}$ s and $\tau_2 \approx 1.2 \times 10^{-6}$ s. By assuming that these time constants correspond to the lifetimes of minority carriers (electrons), we estimated the mobility of electrons from the products $\mu_n\tau_n \approx 8.3 \times 10^{-5}$ and $\approx 4.1 \times 10^{-5}$ cm^2/V, which were determined in portions *3* and *4* of the current–voltage characteristic, respectively. In this case, we obtained the values $\mu_{n1} \approx 95$ cm^2/V s and $\mu_{n2} \approx 60$ cm^2/V s for portion *3* and $\mu_{n1} \approx 45$ cm^2/V s and $\mu_{n2} \approx 34$ cm^2/V s for portion *4* of the current–voltage characteristics. The estimated values of μ_n are within the reasonable limits for these materials. The fact that, in the photoconductivity relaxation curves, there are two or more relaxation time constants and their change in magnitude depending on the current density suggest that the recombination processes occur simultaneously in several channels. Therefore, for a specified injection level, the activity in the recombination processes is manifested by a particular type of recombination centers, which, most likely, consist of complexes into which the charge carriers are trapped, because the base of the structure (p-CdTe) under investigation is a high-resistivity compensated material containing complexes of the type $(V_{Cd}^{2-}D^+)^-$, $(V_{Cd}^{2-}Te_i^*)^{2-}$, etc.

Further, we will discuss the reliability of the electrical resistivity ρ estimated in portions *3* and *4* of the current–voltage characteristics. A comparison of these data with the initial resistivities of the films demonstrates that they are more than half-order of magnitude smaller. This difference in the values is explained by changes in the parameters of the recombination processes occurring in p-CdTe layers during the emission of electrons from the metal (Al) into the semiconductor, as well as by the errors in the measurements of the base thickness d and the surface area of the structure S.

3.2. Analysis of the Reverse Branch of the Current–Voltage Characteristics

Let us now analyze the behavior of the reverse branch of the current–voltage characteristic of the Al–p-CdTe–Mo structure. This structure at a reverse bias can be used as a detector of nuclear particles with a short mean free path, such as alpha-particles, nuclear fragments, etc. The detection of nuclear particles in detectors occurs in space charge layers. The geometrical dimensions of the space charge, especially the thickness and leakage currents at a rectifying junction, as well as the properties of the ohmic contact, play a decisive role in the formation of spectrometric parameters of the detectors. Therefore, it is of particular interest to investigate the electronic processes occurring in space charge layers formed in the base layers of the Schottky barriers with different electrical resistivities. It is also interesting to investigate the influence of the properties of the rear ohmic contacts on these electronic processes.

The current–voltage characteristic of a typical reverse-biased Schottky barrier diode (Al–p-CdTe–Mo) is plotted on a log–log scale in Fig. 5. The base of this structure p-CdTe has a resistivity $\rho \approx 10^5\ \Omega$ cm, and the area of the metal contact (Al) is equal to ~1 cm^2. As can be seen from Fig. 5, the current–voltage characteristic consists of four portions, which are described by the following dependences of the current on the voltage: (*1*) $I = AV^{\alpha_1}$, $\alpha_1 = 0.6$; (*2*) $I = AV^{\alpha_2}$,

TIB HANNOVER +495117628998 Tue Jan 6 16:57:41 2015 Seite 8 von 14

$\alpha_2 = 2$; (*3*) $I = AV^{\alpha_3}$, $\alpha_3 = 1$; and (*4*) $I = AV^{\alpha_4}$, $\alpha_4 = 2$. In portion *1* of the current–voltage characteristic, the current as a function of the voltage varies according to the law $I \sim V^{1/2}$. This dependence of the current on the voltage is observed when the width of the space charge region increases with an increase in the reverse voltage [15]. When the Schottky barrier diode is switched on in the reverse direction, the reverse current density (it is assumed that $\tau_0 = \tau_n = \tau_p$) can be written in the form [15]

$$I_0 = qL_n(n_p/\tau_n) + qd(n_i/2\tau_0). \quad (12)$$

The first term of expression (12) describes the current induced by thermal generation of charge carriers at the rate n_p/τ_n in the base layer with the width L_n in the rear of the space charge region (I_{sat}), and the second part of expression (12) describes the current induced by the generation of charge carriers in the space charge region. Since the space charge region is depleted in carriers, we have $pn \le n_i^2$, and the Shockley–Read statistics [21] can be written as $r - g = -n_i/2\tau_0$; i.e., at a reverse bias, the generation of charge carriers in the space charge region dominates over the recombination. In semiconductors with a large band gap, for example, in silicon, gallium arsenide, and cadmium telluride, the value of n_i is small; therefore, the current induced by the generation of charge carriers dominates. The ratio between the two current components in expression (12) is given by

$$I_{rec}/I_{sat} = dn_i/2n_pL_n = dn_p/2n_iL_n. \quad (13)$$

This ratio increases with a decrease in the temperature and a decrease in the parameters τ, and L_n.

Next, we write the generation current in the form [15]

$$I_r = \frac{n_i}{2\tau_0}\left(\frac{2q\varepsilon\varepsilon_0}{N_{A,\,\mathrm{eff}}}\right)^{1/2}\varphi_k - \frac{n_i}{2\tau_0}\left(\frac{2q\varepsilon\varepsilon_0}{N_{A,\,\mathrm{eff}}}\right)^{1/2}V^{1/2}, \quad (14)$$

where ε and ε_0 are the permittivities of the semiconductor and vacuum, respectively; $N_{A,\,\mathrm{eff}} = N_A - N_D$ is the effective concentration of charged acceptor centers; and φ_k is the contact potential difference. From the slope of straight line *1* in Fig. 5, we determine the lifetime of nonequilibrium charge carriers according to the following expression:

$$\tau_0 = \frac{n_i(2q\varepsilon\varepsilon_0)^{1/2}(V_2^{1/2} - V_1^{1/2})}{2N_{A,\,\mathrm{eff}}^{1/2}(I_{r_2} - I_{r_1})}. \quad (15)$$

The values thus obtained for the lifetimes of nonequilibrium charge carriers are as follows: $\tau_{01} \approx 4 \times 10^{-8}$ s for $N_{A,\,\mathrm{eff}} = 4 \times 10^{13}$ cm^{-3} and $\tau_{02} \approx 1.7 \times 10^{-8}$ s for $N_{A,\,\mathrm{eff}} = 9.1 \times 10^{13}$ cm^{-3}. The effective concentration of charged acceptor centers was determined from the steep portion of the capacitance–voltage dependence $C^{-2}(V)$ of the Schottky barrier diode (Fig. 6), which

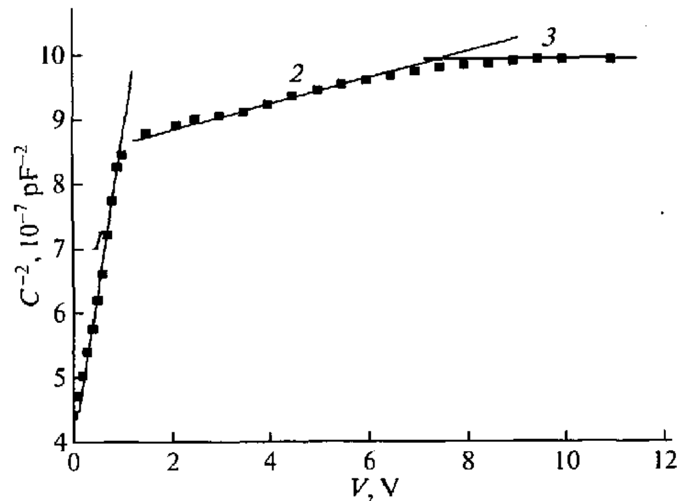

Fig. 6. Capacitance–voltage characteristic of a reverse-biased Schottky barrier diode ($\rho \approx 10^5\ \Omega$ cm) at a frequency $f = 100$ kHz. Numerals indicate different portions of the dependence.

has an inflection and consists of two straight lines. This indicates the heterogeneity of the near-surface layer of the *p*-CdTe film. The values of $N_{A,\,\mathrm{eff}}$ obtained from these straight-line dependences of C^{-2} on V were used to estimate the values of τ_{01} and τ_{02}. These values of the lifetimes of nonequilibrium charge carriers are in agreement with the data available in the literature [18] for the lifetimes of charge carriers in CdTe with intrinsic conductivity. These results confirm that, in portion *1* of the reverse current–voltage characteristic, the current is actually limited by the generation of charge carriers in the space charge layer, and the contribution to it from the current I_{sat} is insignificant. Following this portion of the current–voltage characteristic is the dependence of the current on the voltage in the form $I = AV^{\alpha_2}$, where $\alpha_2 = 2$. The current–voltage characteristic of this type can take place in long diodes at low and high injection levels of minority charge carriers. Consequently, in the base of these diodes, the electroneutrality is ensured at every point. However, the Schottky barrier diodes under investigation are switched on in the reverse direction, and their space charges have a sufficiently large thickness. For example, the studied sample at the bias voltage $V = -10$ V has a space charge thickness ~8 μm, which does not change with a further increase in the voltage. Therefore, it is assumed that the nonequilibrium electrons are injected into the space charge layer. The injection of electrons into the space charge layer can occur from interlayers of the grain boundary (as in [22]) or from the rear molybdenum contact when a negative bias is applied to it. The X-ray powder diffraction analysis demonstrated that between the CdTe film and the molybdenum substrate, there is an oxide layer of MoO_3 [23], which is a wide-band-gap semiconductor

with n-type conductivity. Therefore, the injection of electrons can occur from this oxide layer into p-CdTe. Let us assume that electrons are injected into the volume of the space charge with a concentration equal to or higher than the concentration n_t; then, there arises an additional space charge of mobile carriers. In this case, the dependence of the current on the voltage can be represented in the quadratic form [24]

$$I = \varepsilon\varepsilon_0\theta V^2/L^3. \quad (16)$$

From the slope of the plot $I \sim V^2$, we obtain $\mu\theta \sim 2 \times 10^{-5}$ cm^2/V s for $\varepsilon = 9.0$ [9], $\varepsilon_0 = 8.85 \times 10^{-14}$ F cm^{-1}, and $L = 8$ μm, which confirms the monopolar injection into a dielectric with a high concentration of traps [24]. Probably, this dielectric is a part of the base layer (p-CdTe) covered by the space charge. Further, the current–voltage characteristic has a portion where the current is linearly dependent on the voltage. The appearance of the linear portion in the current–voltage characteristic, most likely, is associated with the fact that the volume of the space charge is filled with injected nonequilibrium electrons. As a result, the resistance of the base part as a whole is leveled. However, in this case, the concentration of nonequilibrium electrons injected from the rear contact (Mo) is still less than the concentration of equilibrium charge carriers in the quasi-neutral part of the base layer of the structure. When the concentration of injected nonequilibrium electrons becomes equal to the equilibrium concentration of electrons in the base, there again appears a quadratic dependence of the current on the voltage, which is described by relationship (16). By using the electrical resistivity determined from the linear portion of the current–voltage characteristic, we can estimate the dielectric relaxation time

$$t_\Omega = \varepsilon\varepsilon_0\rho \approx 10^{-4}\ \text{s} \quad (17)$$

for the dependence $I \sim V^2$. According to the estimates, the time required to establish the compensation process in the base is long enough, and the transit time becomes short. Therefore, the injected electrons have no time to "dissipate"; consequently, these arises a space charge of free nonequilibrium charge carriers. It is known [24] that, when the concentration of free electrons is doubled as a result of the injection, the expression for the concentration of nonequilibrium electrons captured into shallow traps takes on the form n_0/θ, and the voltage of transition from the Ohm's law to the quadratic law is determined by the expression [24]

$$V_x = en_0L^2/\theta\varepsilon. \quad (18)$$

In this case, the total concentration of injected electrons is given by $n + n_t \approx n_t$, where n_t is the concentration of electrons captured into traps, and the effective drift mobility is defined as $\mu_{\text{eff}} = (n/n_t)\mu$. By using the definition of the effective drift mobility μ_{eff} and the equation $n/n_t = \rho/\rho_t = \theta$, it is easy to verify that formula (18) is equivalent to the expression

$$t_{x,\text{eff}} = t_\Omega, \quad t_{x,\text{eff}} = L^2/\mu_{\text{eff}}V_x, \quad \mu_{\text{eff}} = (n/n_t)\mu, \quad (19)$$

where $t_{x,\text{eff}}$ is the effective time of flight of the total injected charge through the high-resistivity semiconductor with the voltage V_x and t_Ω is the dielectric relaxation time defined by expression (17). Then, using the equality $t_{x,\text{eff}} = t_\Omega$ (see formula (19)), we find the effective electron mobility $\mu_{\text{eff}} \approx 2 \times 10^{-3}$ cm^2/V s for the parameters $L = 30$ μm and $V_x \approx 4.5$ V. The effective mobility was also determined from portion *2* $I \sim V^2$ according to formula (16): $\mu_{\text{eff}} \approx 1.4 \times 10^{-3}$ cm^2/V s. A comparison of the mobilities μ_{eff} determined from the value of V_x and from the dependence $I \sim V^2$ demonstrates that the base of the Schottky barrier diode under investigation actually has a large number of shallow attachment levels. The capture into these levels increases with an increase in the concentration of injected nonequilibrium charge carriers. This also confirms that the majority of the injected electrons are trapped into the attachment levels.

The injection of nonequilibrium charge carriers into the base of the reverse-biased Schottky barrier diodes is of fundamental importance, because they can determine the noise and functional characteristics of semiconductor devices, in particular, nuclear radiation detectors. Thus, it is interesting to investigate the Schottky barrier diodes in which the base is completely covered by the space charge. Therefore, the Schottky barrier diodes were fabricated on higher resistivity films ($\rho \approx 5 \times 10^6$–$10^7$ Ω cm) with a small surface area $S \approx 7 \times 10^{-2}$ cm^2 of the metal contact (Al). In these structures, the probability of expansion of the space charge layer is rather high. In this case, the possibility of injection of nonequilibrium electrons from interlayers at the grain boundaries into the space charge layer decreases because the number of grain boundaries on the surface area of ~0.07 cm^2 is substantially smaller (~1 cm^2). Furthermore, an increase in the electrical resistivity of the cadmium telluride films leads to an increase in the probability of the formation and accumulation of free tellurium atoms on the surface of crystallites that readily form the TeO_2 compound, which is a good insulator and encourages the passivation of grain boundaries.

The current–voltage characteristic of a typical reverse-biased Schottky barrier diode based on p-CdTe with a base resistivity $\rho \approx 3 \times 10^7$ Ω cm is shown in Fig. 7. As can be seen from Fig. 7, the current–voltage characteristic of the reverse-biased Schottky barrier diode consists of the following four portions: (*1*) $I = AV^{\alpha_1}$, $\alpha_1 \approx 0.59$; (*2*) $I = AV^{\alpha_2}$, $\alpha_2 \approx 1$; (*3*) $I = AV^{\alpha_3}$, $\alpha_3 \approx 2$; and (*4*) $I = AV^{\alpha_4}$, $\alpha_4 \approx 3.8$. In portion *1* of the current–voltage characteristic, the current is limited

TIB HANNOVER +495117628998 Tue Jan 6 16:57:41 2015 Seite 10 von 14

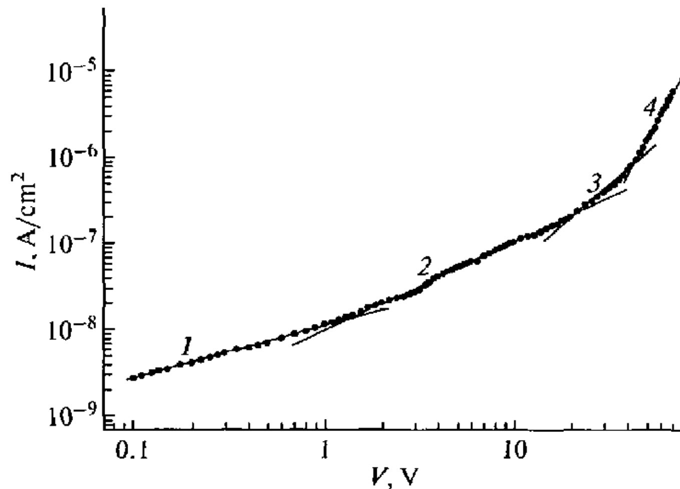

Fig. 7. Current–voltage characteristic of a reverse-biased Schottky barrier diode ($\rho \approx 3 \times 10^7$ Ω cm and $S \approx 0.07$ cm^2) on a log–log scale: (*1*) $I \sim V^{0.59}$, (*2*) $I \sim V$, (*3*) $I \sim V^2$, and (*4*) $I \sim V^{3.8}$.

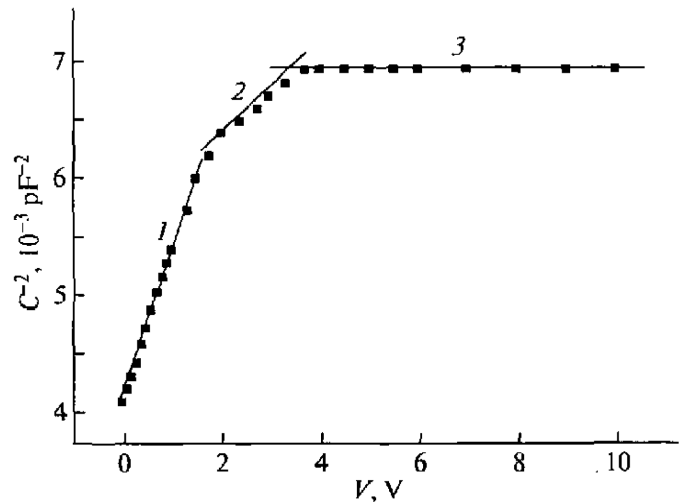

Fig. 8. Capacitance–voltage characteristic of the sample with a base resistivity $\rho \approx 3 \times 10^7$ Ω cm in the C^{-2}–V coordinates at a test signal frequency f = 100 kHz. Numerals indicate different portions of the dependence.

by the generation current in the space charge layer, because the current–voltage characteristic is satisfactorily described by the second term of expression (14), and the capacitance decreases with an increase in the reverse voltage (Fig. 8), which confirms the expansion of the space charge layer. This capacitance–voltage characteristic reaches saturation (plateau) at voltages of ~3–4 V. This means that the space charge already at these voltages completely covers the entire thickness of the base (p-CdTe) of the structure. On the plateau of the capacitance–voltage characteristic, we have the capacitance $C \approx 12.2$ pF, and the evaluation of the thickness of the space charge layer from this value according to the parallel-plate capacitor formula $C = \frac{\varepsilon\varepsilon_0 S}{d}$ gives $d \sim 45.7$ μm. This value almost completely coincides with the thickness of the p-CdTe film: L = 46 μm. Let us assume that, in this portion of the current–voltage characteristic, the current is limited by the generation current. Then, using the second part of formula (14), we calculated the lifetime of equilibrium charge carriers $\tau_0 \sim 5 \times 10^{-7}$ s for the parameters $n_i \approx 10^6$ cm^{-3}, $\varepsilon = 9$, $\varepsilon_0 = 8.85 \times 10^{-14}$ F/cm, $S = 0.07$ cm^2, and $N_{A,\,\mathrm{eff}} = 2.1 \times 10^{12}$ cm^{-3}. For $N_{A,\,\mathrm{eff}} = 3.5 \times 10^{12}$ cm^{-3}, we obtained $\tau_0 \sim 3.3 \times 10^{-7}$ s. The appearance of two values τ_0 is associated with two concentrations of charged local immobile centers. These centers were identified from the rapidly decreasing portion of the dependence $C^{-2}(V)$, which consists of two straight lines (Fig. 8), thus indicating the heterogeneity of the base layer of the p-CdTe film structure. Furthermore, the obtained results have demonstrated that, with an increase in the base resistivity of the structure, the lifetime of equilibrium charge carriers increases; consequently, the concentration of unoccupied recombination centers decreases. For example, when the base resistivity ρ increases from 10^5 Ω cm to $\sim 3 \times 10^7$ Ω cm, the lifetime τ_0 increases from 4×10^{-8} to 5×10^{-7} s.

Following this portion is the portion of the current–voltage characteristic in which the current linearly depends on the voltage. Since the entire thickness of the base of the structure is completely covered by the space charge, the current in this portion of the current–voltage characteristic is limited only by thermal generation of charge carriers. Of course, in this case, the concentration of nonequilibrium electrons injected from the rear contact of the structure is substantially lower than the concentration of thermal equilibrium carriers. When the concentration of injected electrons becomes equal to the concentration of thermal equilibrium electrons, in the current–voltage characteristics there appears a quadratic dependence of the current on the voltage, which is actually observed in the experiment at the voltage $V_{\mathrm{sample}} \approx 18$ V (Fig. 7, curve *3*). From the portion of the quadratic dependence of the current on the voltage, the effective electron mobility μ_{eff} was determined using the value of V_x. First, the mobility μ_{eff} was determined from the value of V_x according to expression (18). As a result, we obtained $\mu_{\mathrm{eff}} \sim 2.1 \times 10^{-3}$ cm^2/V s for the following parameters: $V_x = 18$ V, $t_\Omega = 3.5 \times 10^{-2}$ s, $L = 46$ μm, and $\rho \approx 3.5 \times 10^{10}$ Ω cm. Here, the electrical resistivity of the p-CdTe film (base) covered by the space charge was estimated from the linear portion of the current–voltage characteristic. The second estimate for the mobility $\mu_{\mathrm{eff}} \sim 3.4 \times 10^{-3}$ cm^2/V s was obtained according to formula (16) from the slope of the dependence $I \sim V^2$. The data obtained are in good agreement and suggest that the vast majority of nonequilibrium electrons are trapped. Since $\mu_{\mathrm{eff}} = (n/n_t)\mu$ (see expression

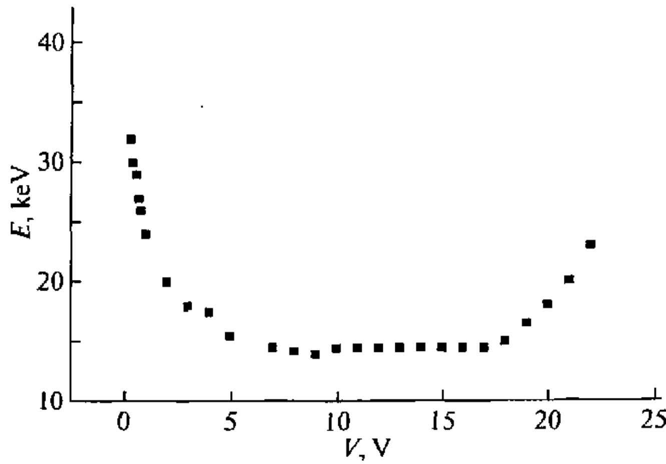

Fig. 9. Dependence of the noise on the voltage at the reverse-biased Schottky barrier diode with a base resistivity $\rho \approx 3 \times 10^7\ \Omega$ cm.

(19)), we have $n_{t1} \approx 2.4 \times 10^4 n$ according to the first estimate of the effective mobility and $n_{t1} \approx 1.5 \times 10^4 n$ according to the second estimate, with the electron mobility $\mu_n \approx 50$ cm^2/V s in the *p*-CdTe films under investigation.

After the dependence $I \sim V^2$ in the current–voltage characteristic (Fig. 7) is the dependence $I \sim V^{3.8}$. The portion with a sharp rise in the current appears upon the unipolar injection [24], when the attachment levels either intersect the quasi-Fermi level or are located at a very short distance from it. The voltage at which the current begins to sharply increase (in the trap filled limit (TFL)) has the form [24]

$$V_{\mathrm{TFL}} \approx \frac{Q_{\mathrm{TFL}}}{C_0} = \frac{ep_{t,0}L}{C_0} \approx \frac{ep_{t,0}L^2}{\varepsilon}. \qquad (20)$$

After substituting the experimental value $V_{\mathrm{TFL}} = 41$ V and $e = 1.6 \times 10^{-19}$ C, $\varepsilon = 9$ for cadmium telluride, $\varepsilon_0 = 8.85 \times 10^{-14}$ F cm^{-1}, and $L = 46$ μm into expression (20), we find that $p_{t,0} \approx 10^{15}$ cm^{-3}. Hence, it follows that the concentration of unfilled traps is high enough, so that a sharp jump in the current–voltage characteristic is not observed. In this case, the ratio of the concentration of unfilled trap centers to the concentration of nonequilibrium free electrons has the form [24]

$$\frac{I(2V_{\mathrm{TFL}})}{I(V_{\mathrm{TFL}})} \approx \frac{p_{t,0}}{n_0}. \qquad (21)$$

After substituting the current $I = 5.6 \times 10^{-8}$ A at the bias voltage $V_{\mathrm{TFL}} = 41$ V and $I = 8.1 \times 10^{-6}$ A with twice the value $V_{\mathrm{TFL}} = 82$ V (Fig. 7, portion *4*) into expression (21), we find the ratio of $\frac{p_{t,0}}{n_0} \approx 145$. This value indicates that the concentration of equilibrium free electrons is $\sim 10^{13}$ cm^{-3}; i.e., it is more than two orders of magnitude smaller than the concentration $p_{t,0}$. The electrons injected from the rear contact will naturally affect the leakage current and noise characteristics of semiconductor devices. As was shown above (Fig. 7), beginning with the voltage $V_x = 18$ V, injected electrons dominate in the charge transfer; consequently, they should also affect other characteristics of the structure. Indeed, the noise of the structure under investigation decreases to the voltage of ~9 V (Fig. 9), remains constant up to 16 V, and then begins to increase. These data confirm that the injection of electrons from the rear contact into the volume of the space charge up to 9 V is almost absent. Further (from 9 to 16 V), there is a weak injection of electrons into the space charge layer and, beginning with the voltage of ~18 V, which corresponds to the transition from the linear portion of the current–voltage characteristic to the quadratic dependence of the current on the voltage, the injected electrons begin to determine the mechanism of charge transfer in the structure and, consequently, the noise significantly increases. This means that the nonequilibrium electrons coming from the rear contact are also responsible for the noise characteristics of the structure under investigation.

Moreover, in the voltage range from 9 to 18 V, the capacitance of the reverse-biased structure is relatively low and constant (~12.2 pF). This behavior of the capacitance–voltage characteristic is explained by the fact that, at these voltages, the effective concentration of charged immobile centers is still considerably higher than the concentration of electrons injected from the rear contact.

4. USE OF THE STUDIED STRUCTURE AS A PHOTOSENSOR

The examination of the structure under investigation as a photosensor is of interest, because the performed analysis of the current–voltage characteristics of the Al–*p*-CdTe–Mo structure has demonstrated that this structure has a high-resistivity base and the ratio of its thickness to the diffusion length lies in the range ~3.5–5.0; furthermore, the studied structure is photosensitive. Therefore, the Al–*p*-CdTe–Mo structure satisfies all the requirements for injection photodiodes [15]. In this respect, we investigated the current–voltage characteristic of the Al–*p*-CdTe–Mo structure under laser irradiation with a wavelength $\lambda = 0.625$ μm and a power density of 83 mW/cm^2 (Fig. 10). As can be seen from Fig. 10, the light current–voltage characteristic differs significantly from the dark current–voltage characteristic in both the forward and reverse current directions. The photocurrent (I_{ph}) substantially exceeds the dark current (I_d) with the same bias voltage. For example, the photocurrent I_{ph} is 15–20 times greater than the dark current I_d at the bias

TIB HANNOVER +495117628998 Tue Jan 6 16:57:41 2015 Seite 12 von 14

voltage $V = 2$ V and it is 100 times greater than that at the bias voltage $V \approx 3.3$ V in the forward current direction. At a reverse bias voltage, the photocurrent at $V_{sh} \approx 0.5$ V almost reaches saturation; in this case, the ratio of I_{ph} to I_d is no less than 10. After that, a further increase in the reverse bias leads to a slow increase in I_{ph}, which is especially pronounced beginning with $V \approx 2$ V.

In order to determine the efficiency of the operation of the structure as a photodiode, we calculated the photocurrent. Under irradiation by laser beams with a wavelength $\lambda = 0.625$ μm and a power density of 83 mW/cm^2, the photon flux $Q_0 = 2.6 \times 10^{17}$ cm^{-2} s^{-1} with an energy $E \approx 1.984$ eV is incident on the surface of the structure. The photon flux in the base (p-CdTe) of the structure according to the calculation using the formula $Q = Q_0S(1 - R)$ is equal to ~9×10^{15} cm^{-2} s^{-1} for $S \approx 7 \times 10^{-2}$ cm^2 (the surface area of the structure) and $R \approx 0.4$ (the fraction of photons reflected from the aluminum interlayer with $E \approx 2$ eV). Now, we assume that all the photons incident on the base are absorbed, and all they form electron–hole pairs that are separated by a barrier without loss. In this case, the generated photocurrent is $I_{ph} = qQ = 1.44 \times 10^{-3}$ A. At the same time, in the experiment we have $I_{ph} \approx 9 \times 10^{-3}$ A at $V = 3.3$ V, which is more than six times higher than the hypothetical calculated values obtained in our work. Hence, it follows that, in this structure, the photocurrent is amplified. This is clearly confirmed by the fact that the current sensitivity of this structure is ~2.6 A/W, whereas the ideal photodetector at this wavelength has a current sensitivity of 0.5 A/W [23], which is more than five times lower. An ideal photovoltaic device is considered to mean a device in which there is no reflection from the surface, the internal quantum efficiency is ~1, and all the generated charge carriers are involved in the formation of the photocurrent.

According to the X-ray diffraction data [23], in the Al–p-CdTe–Mo structure, an interlayer of aluminum oxide (Al_2O_3) with a thickness of ~200 Å is formed between the Al and p-CdTe layers and an interlayer of molybdenum oxide with a thickness of ~300 Å is formed between the p-CdTe and Mo layers. Therefore, this structure can be represented as a structure with two Schottky barriers switched on in the opposing directions. Moreover, these Schottky barriers are technologically connected with the p-CdTe base layer. Let us now analyze what occurs in this structure under irradiation by laser beams with $\lambda = 0.625$ μm. The absorption of photons occurs in the near-surface p-CdTe layers with a thickness of the order of one micrometer, because the Al layer has a thickness of ~50 Å, the intermediate layer between Al and p-CdTe has a thickness of approximately 200–250 Å, and the coefficient of absorption of these photons in CdTe is equal to ~10^4 cm^{-1}. Hence, it follows that nonequilibrium photocarriers are located at a distance of ~1–2 μm from the Al–p-CdTe interface. In this case, the negative potential applied to the Al contact, leads to the formation of a space charge at the Al_2O_3–p-CdTe interface due to the accumulation of nonequilibrium holes, which, in turn, increases the potential barrier. An increase in the concentration of nonequilibrium electrons due to the photogeneration creates an additional gradient of the concentration of minority charge carriers in the p-CdTe layer, which is responsible for the increase in the diffusion current. This leads to a modulation of the resistance of the base region. Since the Schottky barrier is connected in series with the base resistor, the change of the latter leads to a variation in the voltage across the Schottky barrier Al–p-CdTe and in the emission current. In turn, this causes a new change in the base conductivity, a new redistribution of the voltage, and a new enhancement of the electron emission from the metal (Al) into the semiconductor (p-CdTe). This ensures a significant increase in the initial photocurrent; i.e., the considered photodiode is a version of the injection photodiode [15]. The injection photodiode is a diode fabricated from the high-resistivity semiconductor. The base length is several times greater than the diffusion displacement length of minority carriers, and the p–n junction is connected in the forward direction. The injection photodiode operates at high injection levels, and the conductivity of the base region is determined by injected charge carriers.

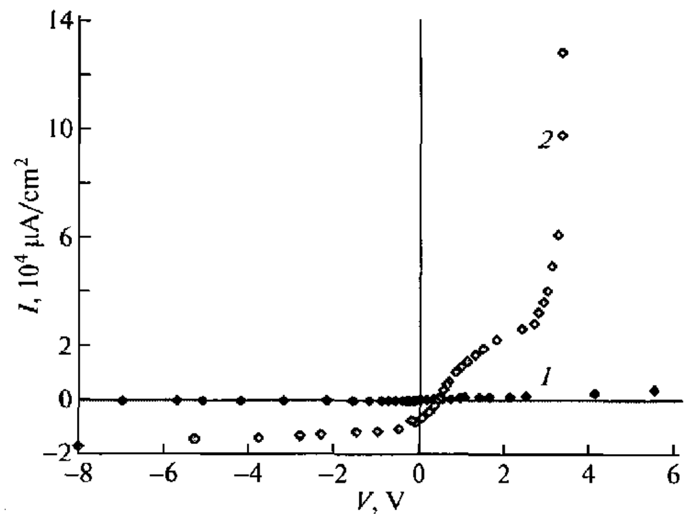

Fig. 10. (*1*) Dark and (*2*) light current–voltage characteristics of the Schottky diode (Al–p-CdTe–Mo) with a base resistivity $\rho \approx 10^7$ Ω cm at room temperature under laser irradiation with a wavelength $\lambda = 0.625$ μm and a power density of 83 mW/cm^2.

Irradiation with light from the fundamental or impurity absorption region leads to a change in the resistance of the base region due to both the direct increase in the charge carrier concentration (as in a

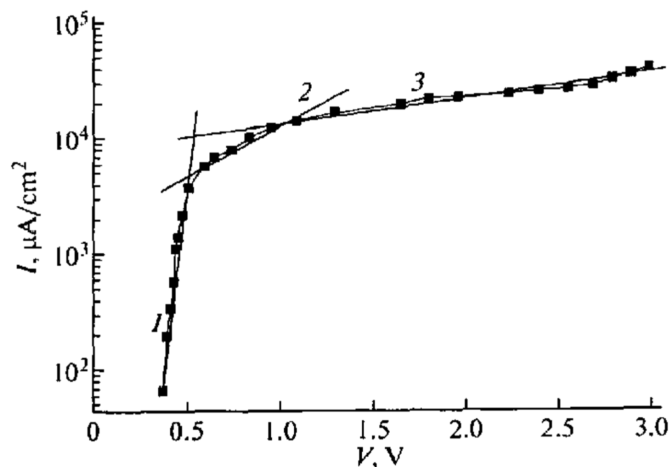

Fig. 11. Forward branch of the light current–voltage characteristic of the Schottky barrier diode (Al–p-CdTe–Mo) with a base resistivity $\rho \approx 10^7$ Ω cm under laser irradiation with a wavelength $\lambda = 0.625$ μm and a power density of 83 mW/cm^2. Numerals indicate different portions of the dependence.

photoresist) and the change in the parameters (such as lifetime and mobility) determining the distribution of nonequilibrium charge carriers in the base region. A change in these parameters leads to a variation in the distribution of nonequilibrium charge carriers and, consequently, the resistance of the base region.

The structure under investigation also has a high-resistivity base region, its thickness is ~3.5–5.0 times greater than the diffusion displacement length of minority carriers, and the concentration of nonequilibrium charge carriers is substantially higher than the concentration of equilibrium charge carriers. Therefore, the structure satisfies all the requirements for injection photodiodes; in this case, the p–n junction is replaced with the Schottky barrier.

In order to elucidate the modulation of the base resistance and the related physical processes, we investigated the light current–voltage characteristic of the structure (Fig. 11). As can be seen from Fig. 11, the light current–voltage characteristic consists of three portions in which the dependence of the current on the voltage is described by the following exponential expressions: (*1*) $I = I_{01}[\exp[qV/c_1kT) - 1]$, where $c_1 = 1.05$ and $I_{01} = 3 \times 10^{-11}$ A; (*2*) $I = I_{02}[\exp[qV/c_2kT) - 1]$, where $c_2 = 16$ and $I_{02} = 9 \times 10^{-5}$ A; and (*3*) $I = I_{03}[\exp[qV/c_3kT) - 1]$, where $c_3 = 80$ and $I_{03} = 6.2 \times 10^{-4}$ A. In portion *1* of the current–voltage characteristic, the dependence of the current on the voltage is described by the thermal electron emission, because the exponent is $c_1 \approx 1.05$. The potential barrier height W estimated from the experimental value $I_{01} = 3 \times 10^{-11}$ A proved to be ~1.02 eV, which is 0.07 eV larger than the value observed in the dark. This fact confirms once more that, after irradiation with laser beams, the potential barrier height increases as a result of the sharp increase in the concentration of nonequilibrium holes at the Al–p-CdTe interface.

Using the experimental values of c in the exponent and the pre-exponential factor I_0 calculated from portions *2* and *3* of the light current–voltage characteristic (Fig. 11), we determined the parameters L_n, $\mu\tau_n$, and ρ from expressions (10) and (11), as was done in the analysis of the dark current–voltage characteristics obtained in the dark. As a result, we obtained the following parameters: $L_n = 14.3$ μm, $\mu\tau_n \approx 8 \times 10^{-5}$ cm^2 V^{-1}, and $\rho \approx 3.5 \times 10^6$ Ω cm for portion *2* and $L_n = 9.7$ μm, $\mu\tau_n \approx 3.7 \times 10^{-5}$ cm^2 V^{-1}, and $\rho \approx 2.6 \times 10^6$ Ω cm for portion *3* of the light current–voltage characteristic. The calculation was carried out using the experimental data ($c_2 = 16$, and $I_{02} = 9 \times 10^{-5}$ A; $c_3 = 80$, and $I_{03} \approx 6.2 \times 10^{-4}$ A) and the geometric data: $d \approx 47$ μm (the thickness of the p-CdTe base) and $S \approx 7 \times 10^{-2}$ cm^2 (the sensitive area of the structure). The analysis of the obtained results has demonstrated that the diffusion displacement length of minority carriers (electrons) and the product $\mu_n\tau_n$ have almost the same values as those obtained from the dark current–voltage characteristic (Fig. 2, portions *3* and *4*). This circumstance suggests that the recombination parameters either remain unchanged or change only slightly. The base resistivity changes as a result of the increase in the concentration of nonequilibrium charge carriers. This is confirmed by the resistivities calculated before (4.7×10^6 and 3×10^6 Ω cm) and after (3.5×10^6 and 2.6×10^6 Ω cm) irradiation.

5. CONCLUSIONS

Thus, the possibility of fabricating a Schottky barrier on Al–p-CdTe structures with the lowest density of surface states has been demonstrated and confirmed by the results obtained from the capacitance–voltage and photoelectric measurements of the potential barrier height. It has been established that, at current densities of 3.3×10^{-7}–5.5×10^{-5} A cm^{-2} in the Al–p-CdTe–Mo structure under investigation, the current is limited by the recombination in the space charge layer. In this case, the calculated lifetime of nonequilibrium charge carriers differs from the experimental value by almost one order of magnitude, which is explained by the recombination processes involving complex centers into which charge carries are trapped. It has been shown that the Al–p-CdTe–Mo structure in the forward direction of the current at high illumination levels operates as an injection photodiode. This injection photodiode has a high current photosensitivity. For example, we have $S_\lambda \approx 2.6$ A/W at the wavelength $\lambda = 0.625$ μm, which is more than five times higher than the spectral sensitivity of an ideal photodetector at this wavelength. It has been established that, in these injection photodiodes, the photocurrent amplification

TIB HANNOVER +495117628998 Tue Jan 6 16:57:41 2015 Seite 14 von 14

occurs as a result of the modulation of the base resistivity with an increase in the concentration of nonequilibrium charge carriers.

It has been shown that, in the Schottky barrier diodes fabricated on coarse-grained p-CdTe films with an electrical resistivity $\rho \approx 10^5$–10^7 Ω cm, even at thermodynamic equilibrium, the space charge has a sufficient thickness: $d \approx 5$ μm at $\rho \approx 10^5$ Ω cm and $d \approx 30$ μm at $\rho \approx 3 \times 10^7$ Ω cm. It has been established that an increase in the degree of compensation (the electrical resistivity ρ of the base) leads to an increase in the lifetime of the equilibrium charge carriers. For example, with an increase in the electrical resistivity ρ of the base from 10^5 to 3×10^7 Ω cm, the value of τ_0 increases from 4×10^{-8} to 5×10^{-7} s. The investigations of the current–voltage, capacitance–voltage, and noise characteristics of the Schottky diodes with the Al–p-CdTe–Mo structure, when the current is switched on in the reverse direction, have demonstrated that, after the complete coverage of the base of the structure by the space charge, electrons responsible for the charge transfer mechanism and noise characteristics of the structure are injected from the rear contact. Apparently, the MoO_3 compound is a source of electron injection. This compound is formed between the film and the molybdenum substrate (according to the data obtained from the X-ray powder diffraction analysis during the growth of p-CdTe). Therefore, it can be concluded that the Al–p-CdTe–Mo structure can be used for detection of nuclear radiation; however, in this case, it is necessary to create a high-quality ohmic contact.

ACKNOWLEDGMENTS

This study was supported by the Fundamental Research Foundation of the Uzbekistan Academy of Sciences (grant no. FA-F032).

REFERENCES

1. T. Takahashi and S. Watanabe, IEEE Trans. Nucl. Sci. **48**, 950 (2001).
2. S. Watanabe, T. Takahashi, Y. Okada, G. Sato, M. Kouda, T. Mitani, Y. Kabayashi, K. Nakazawa, Y. Kuroda, and M. Onishi, IEEE Trans. Nucl. Sci. **49**, 210 (2002).
3. T. Tanaka, T. Kabayashi, T. Mitani, K. Nakazawa, K. Oonuki, G. Sato, T. Takahashi, and S. Watanabe, New Astron. Rev. **48**, 309 (2004).
4. L. A. Kosyachenko, V. M. Sklyarchuk, O. L. Maslyanchuk, E. V. Grushko, V. A. Gnatyuk, and Y. Hatanaka, Tech. Phys. Lett. **32** (12), 1056 (2006).
5. H. Hermon, M. Shieber, and R. B. James, J. Electron Mater. **28**, 688 (1999).
6. *Polycrystalline Semiconductors*, Ed. by G. Harbeke (Springer, New York, 1985; Mir, Moscow, 1989).
7. J. Janabergenov, Sh. A. Mirsagatov, and S. Zh. Karazhanov, Inorg. Mater. **41** (8), 800 (2005)
8. L. W. Davies, Proc. IEEE **51**, 1637 (1963).
9. A. L. Fahrenbruch and R. H. Bube, *Fundamentals of Solar Cells* (Academic, New York, 1983; Energoatomizdat, Moscow, 1987).
10. S. Sze, *Physics of Semiconductor Devices* (Wiley, New York, 1981; Mir, Moscow, 1984), Vol. 1.
11. *Physics and Chemistry of II–VI Compounds*, Ed. by M. Aven and J. S. Prener (North-Holland, Amsterdam, 1967; Mir, Moscow, 1970).
12. A. Milnes and D. Feucht, *Heterojuctions and Metal-Semiconductor Junctions* (Academic, New York, 1972; Mir, Moscow, 1975).
13. V. G. Georgiu, *Capacitance–Voltage Measurements of Parameters of Semiconductors* (Shtiintsa, Chisinau, 1987) [in Russian].
14. Sh. A. Mirsagatov and O. K. Ataboev, in *Proceedings of the Conference "Fundamental and Applied Problems of Physics," Tashkent, Uzbekistan, 2010*, p. 226.
15. I. M. Vikulin and V. I. Stafeev, *Physics of Semiconductor Devices* (Sovetskoe Radio, Moscow, 1980) [in Russian].
16. A. Yu. Leiderman and M. K. Minbaeva, Semiconductors **30** (10), 905 (1996).
17. M. G. Sheinkman and N. E. Korsunskaya, in *Physics of II–VI Compounds*, Ed. by A. N. Georgobiani and M. K. Sheinkman (Nauka, Moscow, 1986) [in Russian].
18. K. Zanio, *Semiconductors and Semimetals* (Academic, New York, 1978).
19. A. Ambrozyak, *Structure and Technology of Semiconductor Photoelectric Devices* (Sovetskoe Radio, Moscow, 1970) [in Russian].
20. V. I. Stafeev, Zh. Tekh. Fiz. **28** (8), 1631 (1958).
21. W. Shockley and W. Read, Phys. Rev. **87**, 835 (1952).
22. Sh. A. Mirsagatov, B. U. Aitbaev, and V. Rubinov, Semiconductors **30** (3), 301 (1996).
23. Sh. A. Mirsagatov, S. A. Muzvfarova, M. S. Baiev, and A. S. Achilov, Uzb. Fiz. Zh. **12** (3), 154 (2010).
24. M. Lampert and P. Mark, *Current Injection in Solids* (Academic, New York, 1970; Mir, Moscow, 1973).

Translated by O. Borovik-Romanova